Journal of Innovative Optical Health Sciences
Vol. 7, No. 1 (2014) 1450017 (9 pages)

DOI: 10.1142/S1793545814500175

A BIOSENSOR USING COUPLED PLASMON WAVEGUIDE RESONANCE COMBINED WITH HYPERSPECTRAL FLUORESCENCE ANALYSIS

CHAN DU[*,‡], LE LIU[†], JUN GUO[*], YONGHONG HE[*,§], JIHUA GUO[*], SHUQING SUN[*] and HUI MA[*,‡]

[*]*Shenzhen Key Laboratory for Minimal Invasive Medical Technologies*
Graduate School at Shenzhen, Tsinghua University
Shenzhen 518055, P. R. China

[†]*Laboratory of Advanced Power Source*
Graduate School at Shenzhen, Tsinghua University
Shenzhen 518055, P. R. China

[‡]*Department of Physics, Tsinghua University*
Beijing 100084, P. R. China
[§]*heyh@sz.tsinghua.edu.cn*

Received 30 May 2013
Accepted 11 September 2013
Published 2 January 2014

We developed a biosensor that is capable for simultaneous surface plasmon resonance (SPR) sensing and hyperspectral fluorescence analysis in this paper. A symmetrical metal-dielectric slab scheme is employed for the excitation of coupled plasmon waveguide resonance (CPWR) in the present work. Resonance between surface plasmon mode and the guided waveguide mode generates narrower full width half-maximum of the reflective curves which leads to increased precision for the determination of refractive index over conventional SPR sensors. In addition, CPWR also offers longer surface propagation depths and higher surface electric field strengths that enable the excitation of fluorescence with hyperspectral technique to maintain an appreciable signal-to-noise ratio. The refractive index information obtained from SPR sensing and the chemical properties obtained through hyperspectral fluorescence analysis confirm each other to exclude false-positive or false-negative cases. The sensor provides a comprehensive understanding of the biological events on the sensor chips.

Keywords: Coupled plasmon waveguide resonance; sensing; hyperspectral fluorescence.

1. Introduction

Surface plasmon resonance (SPR) sensor is the most commercially successful optical sensor[1,2] that could be utilized in a wide range of fields from fundamental researches[3,4] to chemical,[5] biological[6] and clinical applications.[7] SPR uses an optical method to measure molecular binding events at the metal surface by recording the variation of resonance position caused by the change of refractive index (RI). Based on the SPR-generated exponential evanescent field, SPR sensors permit the applications in chemical or biological researches with the advantage of labeling free, high sensitivity, low background disturbance and real-time analysis of dynamical reaction process.[8]

The last two decades have witnessed remarkable progress[9,10] in the development of SPR sensors in the area of both basic concepts and application fields.[11,12] However, this technology also demonstrates the intrinsic limitations[13] in sensitivity, resolution and penetration depth which is usually lower than 300 nm. Considerable efforts have been taken to substantially enhance the performance of sensitivity and resolution of the SPR sensors.[14–16] One of the promising strategies to improve the performance of SPR sensors is adding dielectric layers to form planar waveguide layers for the generation of guided modes in the SPR substrate.[17,18] The resonances between guided light modes within the waveguide layer and surface plasmon polarizations (coupled plasmon waveguide resonance, CPWR) leads to narrower full width half-maximum (FWHM) of the reflective curves and this in turn leads to increased resolution of the sensors by reducing the uncertainty of the resonance position. Besides, theoretical results indicate that CPWR also results in better performance no matter for detection range or for enhanced electromagnetic field[19] which is highly suitable for background excitation of fluorescence to maintain an appreciable signal-to-noise ratio.

Our work in this paper proposes an implementation of symmetrical metal-dielectric structure (MgF_2–Au–MgF_2) to afford CPWR as a possible improvement to conventional SPR systems. Calculated and experimental results substantiate that this structure results in better resolution for no matter fluid or atmosphere analyte.[20] To demonstrate the biomedical applications of symmetrical CPWR-based SPR biosensor, we functionalize the sensor surface by coating dopamine film and a cellular mediator of platelet derived growth factor (PDGF) presented in human aqueous humor samples is detected. This symmetrical CPWR biosensor is further advanced by taking advantage of the strong surface enhanced evanescent field to excite fluorescence at a dark background style. The hyperspectral fluorescence technique is employed to record the full fluorescence spectra and this in turn makes it possible for the separation of multiple fluorescent tags. It is believed that this new biosensor based on CPWR will exhibit enormous potential in the development of optical biosensors.

2. Materials and Methods

2.1. *Materials*

Glucose powder purchased from Aladdin (China) was dissolved into deionized water and distilled to different concentrations for use. Dopamine was also bought from Aladdin (China). Phosphate-buffered saline (PBS), bovine serum albumin (BSA) and Tris were acquired from Sigma (USA). The human anti-PDEF was purchased from R&D Systems Inc. (USA). Fluorescence tags of Cy5 (absorption/emission: 649/667nm) and dylight680 (absorption/emission: 680/715nm) were purchased from Zibo Yunhui Bio-technology Co., Ltd and the EARTH, Inc., respectively.

2.2. *Sensor chip*

Figure 1(a) shows the 1D implementation of the conventional SPR (left) and the symmetrical (MgF_2–Au–MgF_2) CPWR (right) that we utilized in this paper. Based on multiple reflectance theory and Frensnel's formulae, the angular distribution of reflectivity [see Fig. 1(b) and 1(c)] and evanescent field distributions [see Fig. 1(e)] could be calculated for this dielectric–metal–dielectric slab style for the excitation of guided waveguide mode. From the theoretical results given in Fig. 1(b), we can figure out that the resonance between the surface plasmon wave and the guided mode that occurs in a small angular region immediately preceding the critical angle when the thickness of the second layer of MgF_2 (attached to the analyte) is thick enough to form a waveguide layer. Besides, with the increase in thickness of the waveguide layer from 620 to 680 nm, the FWHM of the resonance curve does not

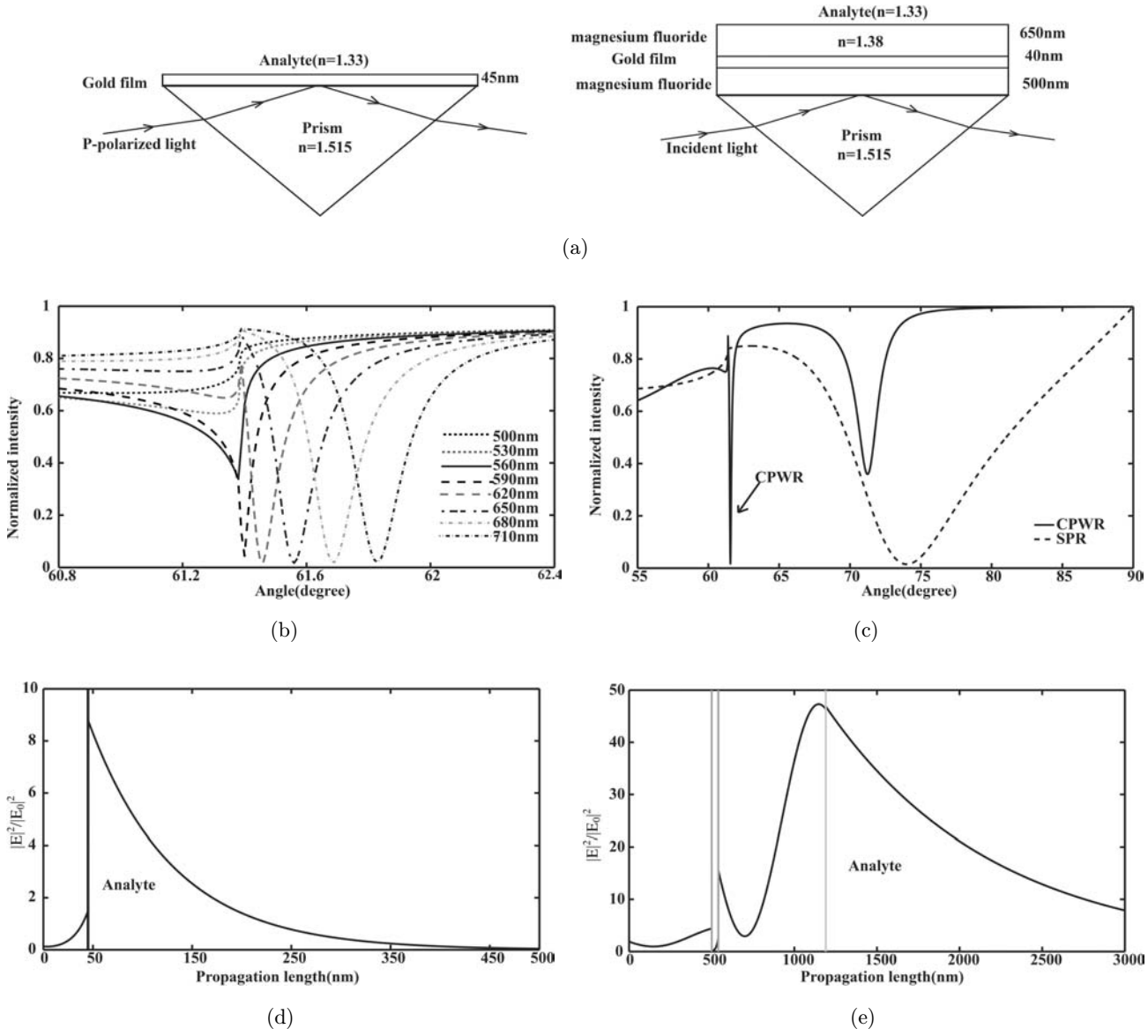

Fig. 1. 1D implementation of conventional SPR ((a) left) and the symmetrical CPWR ((a) right.) (b) Theoretically calculated CPWR under different thicknesses of the waveguide layer. Theoretically calculated reflective curves and electric field distributions excited by conventional SPR (dashed curve in (c), (d) and CPWR (solid curve in (c), (e))). The excitation wavelength is 632.8 nm. Refractive indices for the prism, analyte, magnesium fluoride and gold film are 1.515, 1.33, 1.38 and 0.3123+3.146i individually.

witness significant change while the resonance angle shifts to a bigger position slightly, which is only about 2×10^{-3} degree/nm, this, means the thickness of MgF_2 layer is not very critical for the occurence of CPWR once it is thick enough to afford waveguide modes. It is also the same case for the first layer of MgF_2 (attached to the glass substrate). Compared with the conventional SPR [shown in Fig. 1(c)], the symmetrical CPWR shows a much narrower resonance dip (about one thirtieth of the traditional SPR dip) which makes it favorable for the improvement in the accuracy of the extraction of the resonance angular during practical applications, thus, leading to improved RI resolution. Meanwhile, the symmetrical CPWR also shows a longer propagation depth of about 2 μm into the sensed medium as well as an appreciable enhanced electromagnetic field. On accounting for these features, CPWR sensors are supposed to improve the performance of the optical sensors to a large degree with expended application fields.

In the present work, a glass substrate (the RI is 1.515) coated with three successive layers of MgF_2–Au–MgF_2 is prepared according to the theoretical

results. MgF_2 film is deposited on the polished glass substrate by evaporation coating and the gold film is prepared by vacuum magnetron sputtering. The chip then is put in a vacuum evaporation facility for the preparation of another MgF_2 layer. Thicknesses of the MgF_2 layers and gold film are measured by Ellipsometry (M-2000 UI, J.A. Woollam Co. Inc., USA) and X-ray diffraction (XRD) separately. The sensor chip is attached to a SF4 prism with RI matching oil for the Kretschmann excitation of CPWR. A microfluidic system is mounted against the sensor surface for the detection of aqueous samples.

2.3. *Design considerations and experimental setup*

For the excitation of CPWR, an angle-interrogation method based on the Kretschmann configuration is utilized to measure the reflective curves as a function of the incident angle. A cylindrical lens is used to focus the incident beam into a line at the surface of the sensor chip and it is useful for simultaneous detection of the multi-channel microfluidic system as the focused line could cover several channels at the same time. Also, the focused light includes a successive range of incident angles and reduces the demand for angle scanning. Meanwhile, the enhanced electromagnetic fields caused by CPWR propagates about 2 μm into the analyte and makes it possible for the background excitation of the fluorophores existed in the microfluidic system. Hyperspectra technology is used to record the whole emission spectra of the fluorescence by using a spectroscopy. This technology makes it possible for the simultaneous capture and identification of partially overlapped emission spectra. Combined with the multivariate data algorithm, the ratios of different emission fluorophores can be determined.

Figure 2 shows the schematic of the experimental setup. A light emitting diode (LED) with an electric power of 3 W is used as the light source. A 10× objective lens is used to focus the light onto a aperture. The light is then passed through a collimation lens and a band-pass filter (E, Thorlabs FL632.8-10, with a central wavelength of 632.8 nm and bandwidth of 10 nm). A polarizer is used to produce p-polarized light for the excitation of CPWR. p-polarized light goes into a cylindrical lens ($f = 50$ mm) and is focused into a line at the surface of the sensor films. Fluorophores that existed in the range of surface enhanced electromagnetic fields are excited under CPWR and the fluorescence emitted from the line-illuminated area are focused by an imaging lens into a spectroscopy. A long-pass filter (98% reflection at $\lambda = 633$ nm) is used to further eliminate the scattered and reflected background light. An area charge-coupled device (CCD) is used to record the whole spectra corresponding to each point in the focused line.

3. Results and Discussions

3.1. *Characteristics of the sensor system*

RI resolution(δ_n) and sensitivity (S_n) are two important factors for SPR sensors. Resolution represents the minimum change in the bulk RI that could be detected and it is defined as:

$$\delta n = \delta O / S_n, \tag{1}$$

where δO is the standard deviation (std) of the sensor output (positions of the resonance angle for angular SPR interrogation).

In our present work, a series of glucose solutions with different concentrations (0.3, 0.6, 0.9, 1.2, 1.5 g/L) are used to demonstrate the sensing characteristics of the CPWR sensor. It has ever been

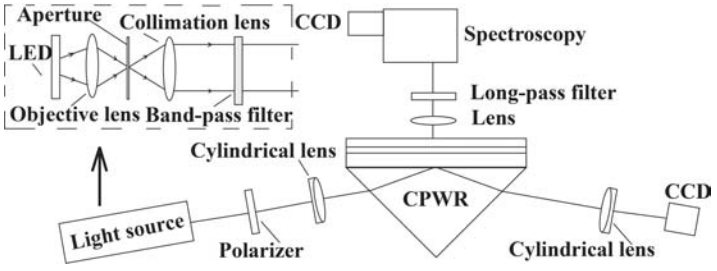

Fig. 2. Schematic of a sensor suitable for simultaneous detections of CPWR and hyperspectral fluorescence analysis.

reported[21] that, the RI of glucose solution could be expressed as a function of its concentration:

$$n = 1.325 + 1.515 \times 10^{-4} \times C, \quad (2)$$

where C refers to the concentration of glucose solution in grams per liter.

Figure 3(a) shows the demonstration of data processing. A two-channel flow cell is mounted against the surface of the sensor chip and the upper channel is filled with deionized water to work as a reference channel. Glucose solutions with different concentrations are pumped into the second channel at a flow rate of 0.5 mL/min. Figure 3(b) exhibits the resonance angular image captured directly by the CCD. The horizontal pixels respond to the angular distributions of the reflected spectra (the linear relationship between the angular and pixel in this work is approximately 1.62×10^{-3} degree/pixel) while the vertical direction represents vertical locations of the sensor chip responding to the illuminated line shown in Fig. 3(a). From the relationship between the resonance positions and concentrations given in Fig. 3(c), it shows an excellent linear relationship between the resonance positions and the concentrations as expected. According to the definition and Eq. (1), a sensitivity of 1.31×10^5 pixels/RIU(212 degree/pixel) can be acquired while the RI resolution of this system is 5.22×10^{-7} RIU. This symmetrical CPWR also shows a wide detection range with an appreciable RI resolution for both fluid and atmosphere analyte.[20]

3.2. *Biomedical applications*

For a dielectric layer that is used as the surface of the CPWR sensor instead of metal films, traditional surface modification methods are not available. In this paper, we refer to an effective way to modify the magnesium fluoride layer with polydopamine film for biological applications.[22] Dopamine is a catecholic (1,2-dihydroxybenzene) compound with a primary amine functional group and it has been proven to be the main composition that responses to the adhesive characteristic of mussels. By immersing substrate in

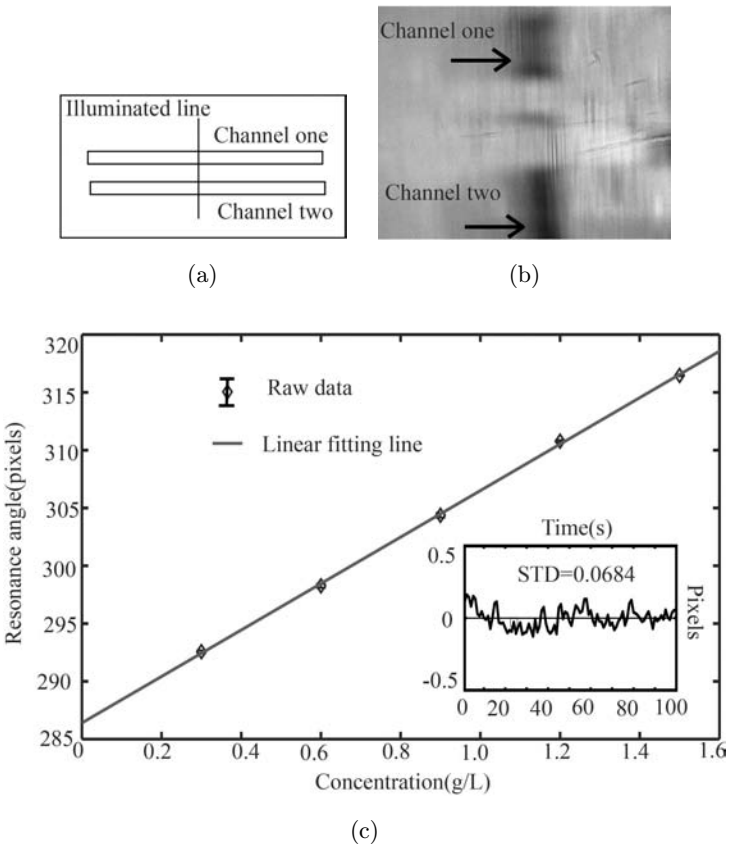

Fig. 3. Sensing characteristics of the system. (a) Structure of the two-channel system. (b) Reflective image captured directly by a CCD. (c) Responses of the resonance angles to glucose solutions with different concentrations (refractive indices). Error bar shows the standard deviation of 100 measurements.

alkaline dopamine solution, adherent polydopamine film will be formed through self-polymerization. The polydopamine film could serve as a multifunctional adhesive layer for a variety of applications.

To demonstrate the biomedical application potential of this system, PDGF, present in human aqueous humor, is detected in this section. PDGF which maintains pericyte viability has been implicated in vessel remodeling *in vivo* and proven to be a potential therapeutic target in the treatment of age-related macular degeneration (AMD).[23] Aqueous humor sample taken from the same patient suffering from AMD are examined to find the variation of PDGF before and after medical therapy treatment in our experiment.

In order to modify PDGF antibody on the sensor surface, polydopamine film is first prepared by dissolving 2 mg dopamine powder in 1 mL tris of 10 mM, pH 8.5. The sensor chip is then immersed into the dilute aqueous solution for about 3 h to form a 15 nm polydopamine film at a dark environment. Polydopamine film on the glass side is washed off and the sensor substrate is attached to a BK7 prism with RI matching oil. A flow cell is then fabricated against the sensor films. Anti-PDGF with a concentration of 10 μg/mL is pumped into the flow channel for 1 h and the unbound molecules are then washed away by a PBS buffer for 20 min. About 0.5% BSA flows through the chamber for an incubation time of 30 min to block the nonspecific sites. About 15 μL aqueous humor is then injected into the flow channel and the interaction process between the PDGF and anti-PDGF is monitored by recoding the shifts of the resonance angles. It can be seen from Fig. 4(c) that

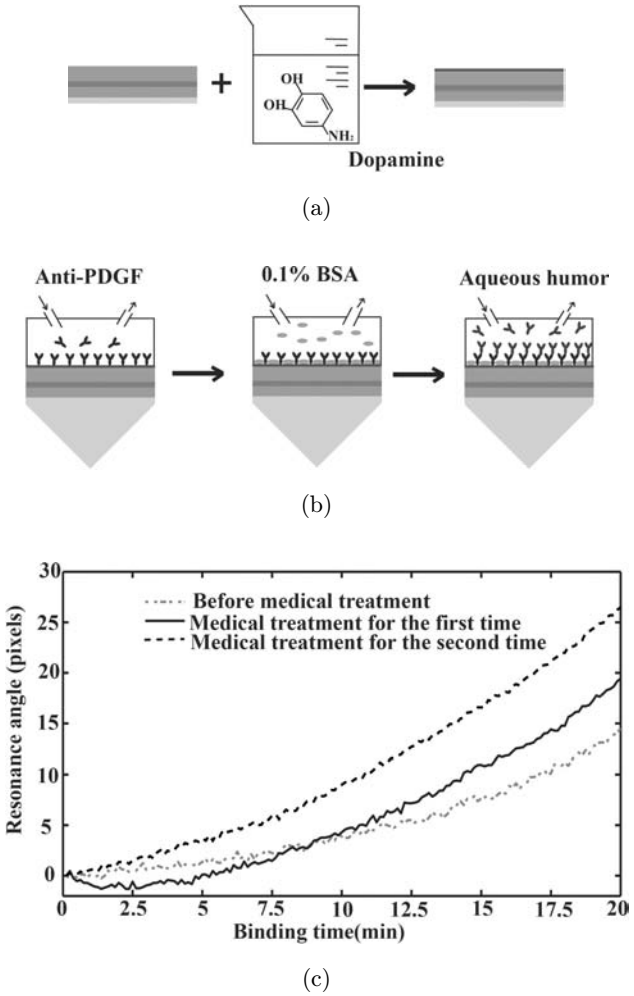

Fig. 4. Biomedical application experiments based on CPWR sensor. (a) Surface modification of the sensor chip by depositing polydopmine films on the MgF_2 layer. (b) Biological procession for the detection of PDGF in aqueous humor samples. (c) Time evolution of the sensing signals (shifts of resonance positions) responding to the binding procedure between PDGF and anti-PDGF.

after a moderate binding process of about 2 min, the samples with medical treatment show bigger binding amounts than the raw sample within the same time frame. The PDGF is believed to be a beneficial factor for the therapy of AMD, hence, it is supposed to exhibit an increased amount after positive treatment and this is consistent with the experimental results. This experiment demonstrates the application approach of our system by providing label-free and real-time detection for medical specimens.

3.3. *Hyperspectral fluorescence analysis*

By taking advantage of the strong surface enhanced electromagnetic field with longer propagation depth generated under CPWR, fluorophores confined in the range of evanescent filed can be excited. By combining the surface plasmon enhance fluorescence technology with the CPWR sensing characteristics, sensitivity of the traditional sensors will be improved by the acquisition of additional chemical information. These two technologies also can confirm each other to exclude false-negative or false-positive cases exited in the experimental process.[24,25]

Different concentrations of Cy5 solutions are used to test the dark field fluorescence excitation ability of this system. A He–Ne laser with a wavelength of 632.8nm and a power of 40 mW is employed as the light source for the sufficient excitation of fluorescence. Figure 5(a) shows the data processing model and the spectrally resolved image captured directly by CCD as shown in Fig. 5(b), corresponding to the illuminated line region in Fig. 5(a). The upper channel is full of Cy5 solution while the second channel is filled with Dylight680 solution. Figure 5(c) shows the normalized fluorescence spec tra against two different concentrations and it can be figured out in Fig. 5(d) that the fluorescence intensities exhibit a linear relationship with the concentrations. Meanwhile, by using the hyperspectra technology, fluorescence tags with overlapping but distinct emission spectra detected at the

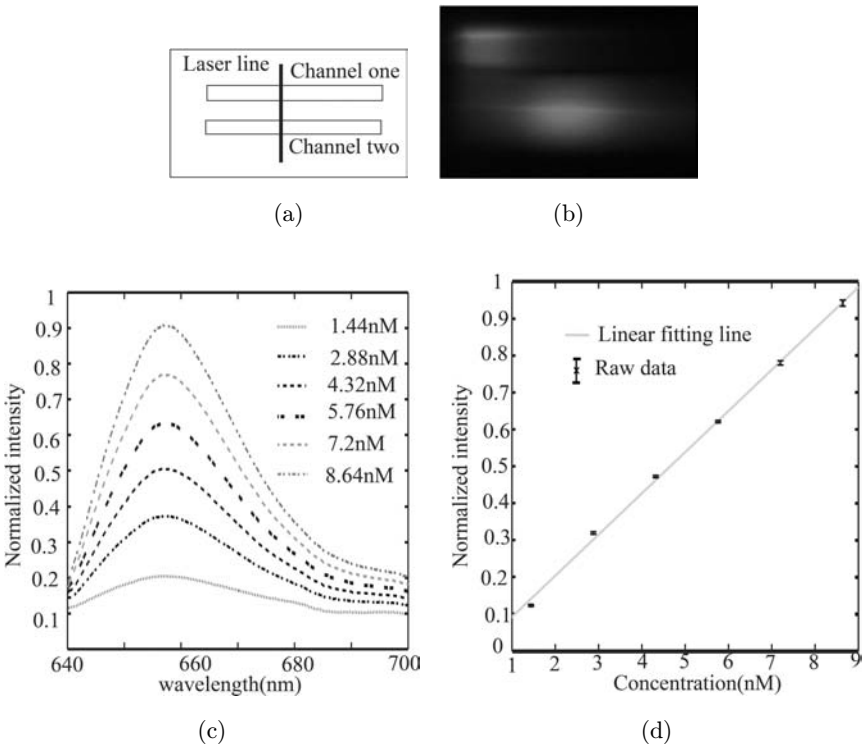

Fig. 5. Hyperspectral fluorescence analysis excited by CPWR. (a) Illustration of the fluorescence excitation model. (b) Raw spectrally resolved image captured by CCD, corresponding to the irradiated line region, the horizontal direction refers to distributions of fluorescence spectra while the vertical direction represents the vertical positions of the flow channels. (c) Fluorescence spectra of Cy5 solutions with different concentrations. (d) Relationship between concentrations and fluorescence intensities acquired by integrating fluorescence spectra at a wavelength range from 650 to 677 nm. (e) Hyperspectral detection and multivariate analysis of the solution mixed with Cy5 and Dylight680. Error bar shows the standard deviation of five measurements.

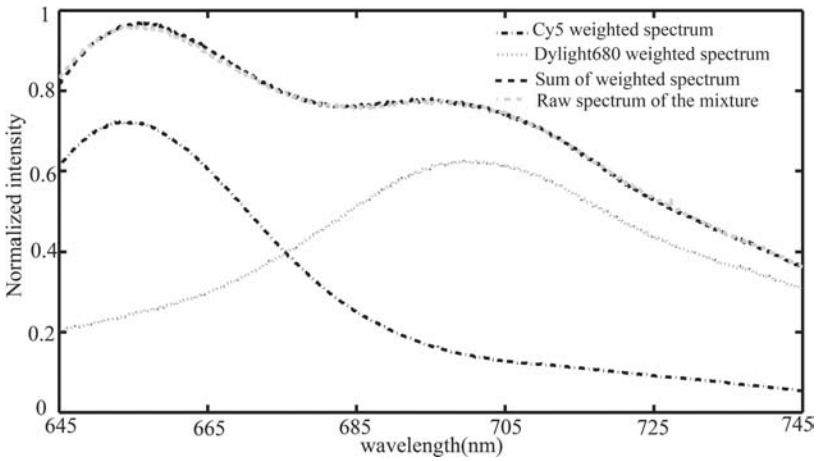

(e)

Fig. 5. (*Continued*)

same time can be distinguished [see Fig. 5(e)] and this in turn leads to increased throughput.

4. Conclusion

In this paper, conventional SPR sensor is advanced by adding dielectric layers on both side of the gold film for the excitation of CPWR. This symmetrical CPWR-based sensor exhibits a high resolution and an extended detection range with appreciable RI resolution. Through a facile approach by depositing polydopamine films to modify the surface of the dielectric layer, the sensor shows its ability for practical biomedical applications with label-free and real-time detections. Meanwhile, sensitivity of the CPWR sensor can be further improved by using the surface enhanced electromagnetic field and the longer propagation length (compared with conventional SPR) for fluorescence excitation at a dark field manner. Combined with hyperspectral technology, different fluorescence emission sources detected simultaneously can be distinguished and throughput ability of the system can be largely enhanced. On account of these features, CPWR sensor is believed to be a promising platform for the comprehensive understanding of biological events on sensor chips.

Acknowledgments

This research was made possible with the financial support from NSFC China (grants 61275188, 81171375 and 61361160416), the key project of Guangdong province (2012A080203008), the Basic Research Program of Shenzhen City (JC201105201121A), State Key Laboratory Open Foundation Issue, China (grant 12K05ESPCT).

References

1. J. Homola, S. S. Yee, G. Gauglitz, "Surface plasmon resonance sensors: Review," *Sens. Actuators B Chemical* **54**(1), 3–15 (1999).
2. J. Melendez, R. Carr, D. Bartholomew *et al.*, "Development of a surface plasmon resonance sensor for commercial applications," *Sens. Actuators B Chemical* **39**(1), 375–379 (1997).
3. S. Herminghaus, P. Leiderer, "Improved attenuated total reflectance technique for the investigation of dielectric surfaces," *Appl. Phys. Lett.* **54**(2), 99–101 (1989).
4. K. Kurihara, K. Suzuki, "Theoretical understanding of an absorption-based surface plasmon resonance sensor based on Kretchmann's theory," *Anal. Chem.* **74**(3), 696–701 (2002).
5. K. Matsubara, S. Kawata, S. Minami, "Optical chemical sensor based on surface plasmon measurement," *Appl. Opt.* **27**(6), 1160–1163 (1988).
6. D. Wassaf, G. Kuang, K. Kopacz *et al.*, "High-throughput affinity ranking of antibodies using surface plasmon resonance microarrays," *Anal. Biochem.* **351**(2), 241–253 (2006).
7. R. L. Rich, Y. S. N. Day, T. A. Morton *et al.*, "High-resolution and high-throughput protocols for measuring drug/human serum albumin interactions using BIACORE," *Anal. Biochem.* **296**(2), 197–207 (2001).

8. J. Homola, "Surface plasmon resonance sensors for detection of chemical and biological species," *Chem. Rev.* **108**(2), 462 (2008).
9. X. D. Hoa, A. G. Kirk, M. Tabrizian, "Towards integrated and sensitive surface plasmon resonance biosensors: A review of recent progress," *Biosens. Bioelectron.* **23**(2), 151–160 (2007).
10. L. He, M. D. Musick, S. R. Nicewarner *et al.*, "Colloidal Au-enhanced surface plasmon resonance for ultrasensitive detection of DNA hybridization," *J. Am. Chem. Soc.* **122**(38), 9071–9077 (2000).
11. H. J. Lee, T. T. Goodrich, R. M. Corn, "SPR imaging measurements of 1-D and 2-D DNA microarrays created from microfluidic channels on gold thin films," *Anal. Chem.* **73**(22), 5525–5531 (2001).
12. K. Usui-Aoki, K. Shimada, M. Nagano *et al.*, "A novel approach to protein expression profiling using antibody microarrays combined with surface plasmon resonance technology," *Proteomics* **5**(9), 2396–2401 (2005).
13. A. A. Kolomenskii, P. D. Gershon, H. A. Schuessler, "Sensitivity and detection limit of concentration and adsorption measurements by laser-induced surface-plasmon resonance," *Appl. Opt.* **36**(25), 6539–6547 (1997).
14. S. Ekgasit, F. Yu, W. Knoll, "Fluorescence intensity in surface-plasmon field-enhanced fluorescence spectroscopy," *Sens. Actuators B Chemical* **104**(2), 294–301 (2005).
15. V. Chabot, Y. Miron, M. Grandbois *et al.*, "Long range surface plasmon resonance for increased sensitivity in living cell biosensing through greater probing depth," *Sens. Actuators B Chemical* **174**, 94–101 (2012).
16. D. Cialla, A. März, R. Böhme *et al.*, "Surface-enhanced Raman spectroscopy (SERS): Progress and trends," *Anal. Bioanal. Chem.* **403**(1), 27–54 (2012).
17. C. W. Lin, K. P. Chen, C. N. Hsiao *et al.*, "Design and fabrication of an alternating dielectric multilayer device for surface plasmon resonance sensor," *Sens. Actuators B Chemical* **113**(1), 169–176 (2006).
18. S. G. Alasaga, N. Cansever, M. M. Aslan, "Sensitivity enhancement of coupled plasmon-waveguide resonance sensors with gold–silver–alumina layers," SPIE Photonics Europe, Int. Society for Optics and Photonics, 84243A-84243A-9 (2012).
19. M. W. Meyer, K. J. McKee, V. H. T. Nguyen *et al.*, "Scanning angle plasmon waveguide resonance Raman spectroscopy for the analysis of thin polystyrene films," *J. Phys. Chem. C* **116**(47), 24987–24992 (2012).
20. H. Shi, Z. Liu, X. Wang *et al.*, "A symmetrical optical waveguide based surface plasmon resonance biosensing system," *Sens. Actuators B Chemical* **185**, 91–96 (2013).
21. J. S. Maier, S. A. Walker, S. Fantini *et al.*, "Possible correlation between blood glucose concentration and the reduced scattering coefficient of tissues in the near infrared," *Opt. Lett.* **19**(24), 2062–2064 (1994).
22. H. Lee, S. M. Dellatore, W. M. Miller *et al.*, "Mussel-inspired surface chemistry for multifunctional coatings," *Science* **318**(5849), 426–430 (2007).
23. J. Yohannan, Y. J. Sepah, Q. D. Nguyen, "Platelet derived growth factor (PDGF) antagonism in neovascular age-related macular degeneration," *Ophthalmology Management* **53**, AMD update (2011).
24. Y. Liu, S. Xu, B. Tang *et al.*, "Note: Simultaneous measurement of surface plasmon resonance and surface-enhanced Raman scattering," *Rev. Sci. Instrum.* **81**(3), 036105 (2010).
25. Z. Liu, L. Yang, L. Liu *et al.*, "Parallel-scan based microarray imager capable of simultaneous surface plasmon resonance and hyperspectral fluorescence imaging," *Biosens. Bioelectron.* **30**(1), 180–187 (2011).